

# Methylbenzenes on graphene

Øyvind Borck

Randaberg videregående skole, Grødemveien 70, NO-4070 Randaberg, Norway

Elsebeth Schröder\*

Microtechnology and Nanoscience, MC2, Chalmers University of Technology, SE-412 96 Göteborg, Sweden

(Dated: July 18, 2016)

We present a theory study of the physisorption of the series of methylbenzenes (toluene, xylene and mesitylene), as well as benzene, on graphene. This is relevant for the basic understanding of graphene used as a material for sensors and as an idealized model for the carbon in active carbon filters. The molecules are studied in a number of positions and orientations relative graphene, using density functional theory with the van der Waals functional vdW-DF. We focus on the vdW-DF1 and vdW-DF-cx functionals, and find that the binding energy of the molecules on graphene grows linearly with the number of methyl groups, at the rate of 0.09 eV per added methyl group.

## I. INTRODUCTION

For environmental safety carbon-based filters play an important role for removal of toxic and hazardous substances, e.g., from the air or drinking or waste water. Smooth, defectless graphene may be used as a simplified model for the active carbon and similar material that is often used as filter material in air and water filters. Although defects and impurities play an important role in how active carbon acts as an adsorbent, already the calculated adsorption energy for adsorption on clean, perfect graphene will be an indication of the strength of the adsorption in the filters [1–4].

At the same time, graphene-based sensors may be used for detection of specific molecules in gases and fluids. The sensor must respond selectively to the various molecules. Both applications thus call for the need of understanding, on a fundamental level, the interaction of a number of molecules with graphene.

Here we focus on the adsorption of the group of methylbenzenes on graphene. We use of density functional theory (DFT) calculations and the method vdW-DF [5–11] to include the long-ranged dispersion interactions that are crucial for physisorption. We find the adsorption energy and the structure (positions of atoms) of the methylbenzenes when adsorbed in isolated positions on graphene.

With the same method, using functionals within the vdW-DF family, we have previously investigated the adsorption of other relatively small but important molecules on to graphene, such as benzene and naphthalene [12], phenol [13], adenine [14] and the other nucleobases [15], chloroform and other trihalomethanes [16], methanol [17], and the first ten of the series of n-alkanes [18], all at low coverage. These and similar results are useful as input for larger-scale force-field molecular dynamics calculations, as well as providing fundamental knowledge on the binding properties at the single molecule level.

The outline for the rest of the paper is as follows: Section II describes methylbenzenes, and Section III describes the method of computation, and the choices made in carrying out the calculations. Section IV reports the results of our calculations, Section V discusses our research results, and finally we summarize the study in Section VI.

## II. METHYLBENZENES

Methylbenzenes is a group of small, aromatic molecules that are volatile and hazardous. They are benzene molecules that have one or more methyl groups attached. We here focus on benzene and the methylbenzenes toluene, para-xylene (1,4-dimethylbenzene) and mesitylene (1,3,5-trimethylbenzene), with one, two, and three methyl ( $\text{CH}_3$ ) groups. The atomic structures are shown in Figure 1. To see the effects of isomers we also study and compare the adsorption energies of xylene with the methyl groups placed closer together: the ortho-xylene (1,2-dimethylbenzene) and meta-xylene (1,3-dimethylbenzene). Trimethylbenzene also exists as the isomers 1,2,3-trimethylbenzene (hemellitene) and 1,2,4-trimethylbenzene (pseudocumene), but these will not be discussed here. In this paper benzene is included as part of the group of methylbenzenes, although strictly taken benzene is not a methylbenzene.

Toluene is a colorless liquid, and is used as raw material for the industry and as a solvent. Toluene is believed to be neurotoxic [19], and thus definitely not suitable neither in drinking water nor should it be inhaled. However, it is still much less toxic than benzene, and thus in some cases replaces benzene as an aromatic solvent. Xylene may also for some applications be used as a solvent even less toxic than toluene.

Graphene is a special material because it consists entirely of surface atoms. The possible amount of adsorbed molecules per volume or weight of carbon is therefore high, compared to other materials with similar adsorption energies per adsorbed molecule.

\* Corresponding author; schroder@chalmers.se

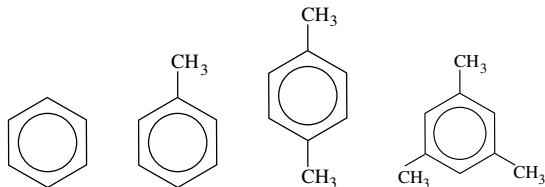


FIG. 1. The atomic structures of benzene, and the methylbenzenes toluene, para-xylene, and mesitylene.

### III. METHOD OF COMPUTATION

The DFT calculations are carried out with the vdW-DF method [5–8, 11] in which the exchange-correlation approximation includes long-range dispersion interactions. We mainly use the versions vdW-DF1 [5, 6] and vdW-DF-cx [9], although we also report some vdW-DF2 [8] results. The vdW-DF1 and vdW-DF2 calculations are carried out with the DFT code GPAW [20, 21] in the Atomic Simulation Environment (ASE) [22, 23]. For calculations using the newer functional vdW-DF-cx [9] we use the DFT code Quantum Espresso (QE) [24, 25] because vdW-DF-cx is not yet implemented in GPAW. All calculations use a fast-Fourier-transform implementation of the central integral in the nonlocal correlation calculations [26].

In all calculations we use periodically repeated orthorhombic unit cells of size  $3\sqrt{3}a_g \times 5a_g = 12.9 \text{ \AA} \times 12.4 \text{ \AA}$  in the lateral plane, and  $23 \text{ \AA}$  in the direction perpendicular to the graphene plane, as illustrated in Figure 2. Here  $a_g = \sqrt{3}a_c$ , where  $a_c = 1.43 \text{ \AA}$  is the C-to-C distance [16] for the present calculations. Each unit cell includes 60 C atoms in graphene and one methylbenzene molecule. By the nature of the DFT calculations the system is in vacuum, and the calculations are carried out at zero temperature.

In the GPAW calculations we use a fast-Fourier transform grid with approximately  $0.12 \text{ \AA}$  between grid points for the wave functions, and half this distance for the electron density. In Ref. [27] we tested the convergence by using only 17% of the grid points for toluene on graphene, along with the restriction to simple  $\Gamma$ -point sampling in  $k$ -space. These rather significant changes to the accuracy resulted in a total of only 20 meV change in adsorption energy, compared to the same calculation carried out at the accuracy used in the present article [27]. The present grid point choices are therefore sufficient.

The sampling of the wave functions and electron density in the QE calculations is given by the energy cutoff values for the wave functions (electron density) 30 Ry (240 Ry), yielding  $0.22 \text{ \AA}$  ( $0.08 \text{ \AA}$ ) between grid points for the wave function (electron density) sampling.

The atomic positions are determined by minimizing the forces acting on the atoms. However, this is only a local optimization that cannot rotate the methyl groups or change the position of the aromatic ring on graphene,

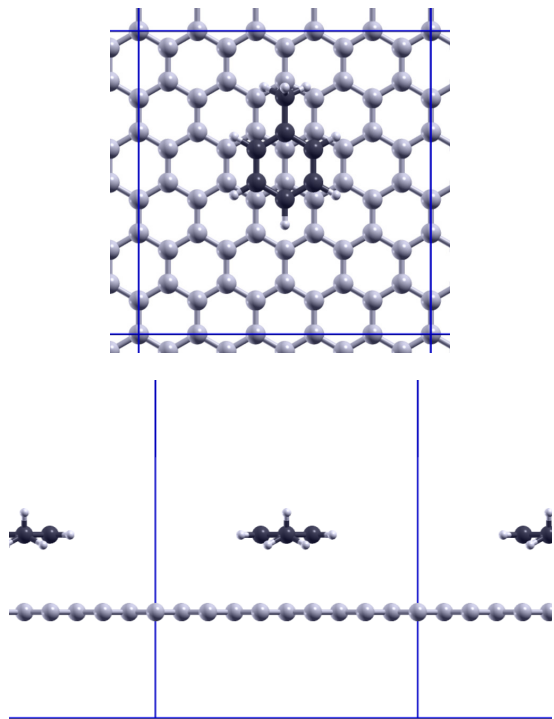


FIG. 2. Sketch of unit cell for toluene adsorption. The height of the unit cell is larger than shown in the lower panel. Light gray spheres are C atoms in graphene, dark gray spheres illustrate C atoms of toluene, and small circles show positions of H on toluene. Shown is the configuration with two H atoms of the methyl group H-tripod pointing towards graphene (‘edge’) and with the center of the aromatic ring positioned on the bridge between two graphene C atoms (‘bridge’).

because the forces are too small, and we therefore use a series of different starting positions and orientation, as illustrated in the supplementary material.

### IV. RESULTS OF THE CALCULATIONS

Our main focus is the calculation of optimal adsorption configurations of the methylbenzenes, and their adsorption energies. For each of the molecules we survey a number of systematically prepared configurations, all of which have their atomic positions further locally optimized, as explained in the previous section.

We define the adsorption energy  $E_a$  as the energy gained by moving the molecule from infinity to its adsorption position near graphene. Binding thus results in a positive value of  $E_a$ . In practice we use the distance  $11.5 \text{ \AA}$  from graphene as the position “far away”. Our study provides adsorption energies, given in Table I and the Supplementary material, as well as the changes in adsorption energies when varying orientations, isomers, and positions relative to graphene.

All adsorption configurations considered, and their

TABLE I. Adsorption energies  $E_a$  for methylbenzenes on graphene, using the functionals vdW-DF1 and vdW-DF2 in DFT program GPAW, and vdW-DF-cx in DFT program Quantum Espresso. Also shown are experimental results from the literature. For some combinations both the configuration with all methyl groups having one H atom pointing towards graphene (‘corner’) and configurations with all methyl groups having two H atoms pointing towards graphene (‘edge’) are shown. Numbers are in units of eV.

	vdW-DF1		vdW-DF2	vdW-DF-cx		Experiments
	corner	edge	edge	corner	edge	
benzene	0.430	0.430	0.386	0.511	0.511	$0.44^b$ , $0.50 \pm 0.08^c$
toluene	$0.498^a$	0.521	0.461	0.599	0.620	$0.52^b$ , $0.71 \pm 0.07^d$
para-xylene	0.557	0.611	0.550	0.666	0.721	
meta-xylene		0.612				
ortho-xylene		0.589				
mesitylene	0.602	0.701	0.632	0.714	0.822	

<sup>a</sup>Originally in Ref. [27].

<sup>b</sup>Ref. [28].

<sup>c</sup>Ref. [29].

<sup>d</sup>Ref. [30].

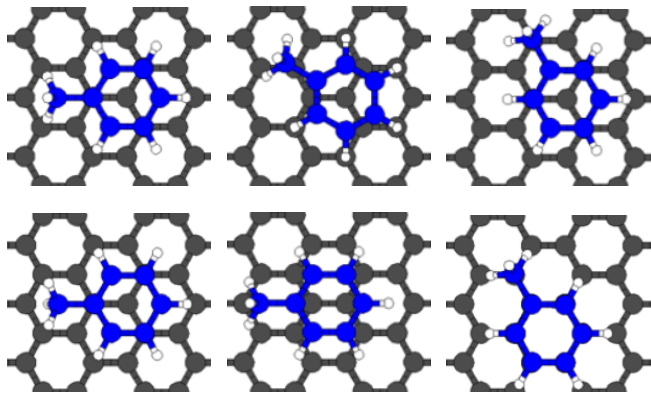


FIG. 3. Examples of various positions of the molecules on graphene, here for toluene. Upper panels show ‘top’ position of the aromatic ring, with the methyl group turned (panels left to right)  $0^\circ$ ,  $30^\circ$ , and  $60^\circ$  around the center of the aromatic ring. The lower panels show ‘top’, ‘bridge’, and ‘hollow’ positions of the aromatic ring. The left lower panel shows the methyl group tripod turned so that a tripod ‘corner’ is directed towards graphene, whereas the upper left panel shows the same configuration, except here a tripod ‘edge’ is directed towards graphene. All atomic positions have been locally optimized by minimizing the remaining Hellmann-Feynman forces on the atoms.

vdW-DF1 adsorption energies, are presented in the Supplementary material. Examples of configurations, for toluene, are given in Figure 3. We study the effects of changing the details of the adsorption configurations on the corresponding adsorption energies, and the trends in the adsorption energies for increasing number of methyl groups in the molecules. As discussed later, molecules like these have been found to adsorb approximately flat on to graphene, when at low coverages [31].

### A. Methyl group H-tripod rotations

Except benzene, all the molecules contain one or more methyl groups. In each methyl group the triangle spanned by the three H atoms can rotate around the axis connecting the methyl group C atom to the aromatic ring. In this work we consider two orientations of the tripod, one where two of the H atoms are closer to graphene than the methyl group C atom, which we term the ‘edge’ configuration (Figure 2), and the ‘corner’ orientation where only one H atom is closer to graphene than the C atom. The two orientations are also illustrated in the two left-most panels of Figure 3.

By comparing the adsorption energies when only the H tripod orientation differs in one or more methyl groups, we find that the ‘edge’ configurations are energetically preferable. We find a remarkably consistent cost for rotating a methyl group from ‘edge’ to ‘corner’: Across eight such pairs of toluene configurations we find that a tripod rotation from ‘edge’ to ‘corner’ carries a cost of 22–28 meV, for para-xylene we find the cost 27 meV per rotated H tripod, and the rotations in mesitylene come at a cost of 28–38 meV per tripod rotation. For mesitylene the cost per rotation increases with the number of tripods already in ‘corner’ orientation, with 28 meV for the first rotation, 32 meV for the next, and 38 meV for rotating also the third tripod from ‘edge’ to ‘corner’ orientation.

### B. Site of aromatic ring

In graphite the formation energy depends on the stacking of the individual layers. Natural graphite is in AB stacking, which means that every other C atom in one layer is placed above a C atom in the neighboring layer, while the other half of the C atoms are above the middle of a ring. It is thus natural, for flat aromatic molecules

TABLE II. Difference in adsorption energies  $E_a$  for methylbenzenes on graphene calculated with vdW-DF1. In all cases we use the best adsorption energy that has the indicated adsorption site and the indicated orientation of all methyl group H tripods. Numbers are in units of meV. All energy differences less than approximately 10 meV are insignificant.

	$E_a^{\text{top}} - E_a^{\text{hollow}}$		$E_a^{\text{top}} - E_a^{\text{bridge}}$	
	corner	edge	corner	edge
toluene	21	17	2	1
para-xylene		21		< 1
meta-xylene		23		3
ortho-xylene		23		7
mesitylene		24		3

like the methylbenzenes, to expect positions that involve placing the aromatic ring either above an atom in graphene ('top' position) or above the middle of a ring in graphene ('hollow' position). For benzene it is known that the 'top' position is preferable [1, 12, 32, 33]. In addition, we also include calculations with the aromatic ring centered on the bridge between two neighboring graphene C atoms ('bridge' position). All positions are illustrated in Figure 3, lower panels.

In most of our calculations we find 'top' sites to be preferable, with the 'bridge' sites close in energy. Distinguishing configurations with H tripod orientations 'edge' or 'corner' we find that for toluene, going from the 'top' to the 'hollow' configuration costs 17–21 meV in adsorption energy, see Table II. The site-change cost is highest for the 'corner' orientation of the tripod. Changing instead from 'top' to the energetically intermediate 'bridge' site yields a vanishing (less than 1 meV) cost. Here, we have chosen the energetically best configurations for the 'top', 'bridge', and 'hollow' adsorption configuration (see Supplementary information for numbers) in the comparison, see Table II.

For the molecules with more than one methyl group the 'bridge' site tends to also be almost as good as the 'top' position, with insignificant energy differences (Table II). The difference in adsorption energy between 'top' and 'hollow' positions is for all the xylenes and for mesitylene around 24 meV or less.

### C. Rotations around the aromatic center

In each adsorption site, the molecule may be rotated around the center of the aromatic ring. For toluene in the 'top' site there are three orientations of the methyl group that carries some symmetry. They are obtained by a 30° and 60° rotation around the aromatic center, as illustrated in the top panels of Figure 3. For the 'hollow' site the 60° rotation is equivalent to the unrotated orientation and thus only two different orientations (none and 30° rotation) are considered. For the 'bridge' site we study both the 30° and 60° rotated configurations, even

though they carry less symmetry than the unrotated configuration, as shown in the middle lower panel of Figure 3. All of these eight configurations for sites 'top', 'hollow', and 'bridge' have two versions, with the 'edge' and the 'corner' orientation of the methyl group H tripod. We find that in all cases, rotation of the molecule around the aromatic center (keeping the H tripod the same) results in energy changes of less than 8 meV, and in most cases even less.

For the xylenes the effect of rotation around the aromatic center is in all cases 7 meV or less. For mesitylene there is no change in energy (< 1 meV) in any of the chosen rotations. Thus, with the effect of rotation being 8 meV or less for all methylbenzenes we find that it is reasonable to ignore the effect of rotations of the molecules.

### D. Optimal adsorption energies

Focusing now on the optimal adsorption energy, irrespective of adsorption site and rotation of the molecule around the aromatic center, we find the adsorption energies listed in Table I.

From Table I we find that as the number of methyl groups in the molecule grows, from benzene to mesitylene, the adsorption energy per molecule also grows. This is shown in Figure 4 for the 'edge' configuration. For dimethylbenzene and trimethylbenzene we use the isomers with evenly distributed methyl groups (para-xylene and mesitylene). In Figure 4 we plot, for each molecule and version of vdW-DF, the highest adsorption energy of all the calculated positions and orientations. The distance of the molecule aromatic center to the graphene plane is similar for all the molecules: approximately 3.6 Å for vdW-DF1, 3.5–3.6 Å for vdW-DF2, and 3.3–3.4 Å for vdW-DF-cx, all for the 'edge' configuration. Distances are slightly larger for the 'corner' configuration. The toluene molecule is adsorbed with the aromatic ring with a small angle (a slight tilt) to the plane of graphene, due to the asymmetry of the toluene molecule.

## V. DISCUSSION OF RESULTS

In the previous section we present adsorption energies for the group of methylbenzene molecules, in several adsorption configurations. We also extract the effects on the adsorption energies when changing the adsorption geometry in various ways, such as rotating the molecule around its aromatic center, rotating the H tripod of the methyl group(s) and translating the molecule along graphene. The vdW-DF1 is constructed with exchange from the revPBE functional [34]. Due to the overly repulsive revPBE exchange, the vdW-DF1 is prone to overestimating the adsorption distances and underestimating binding energies. In vdW-DF2 the inner functional [35] is replaced with the goal of working better

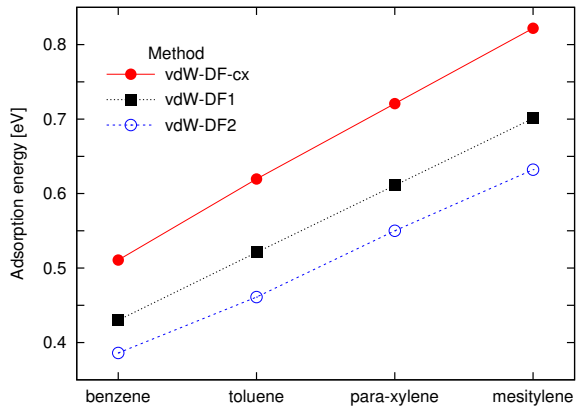


FIG. 4. Adsorption energy of benzene, and the methylbenzenes toluene, para-xylene, and mesitylene, calculated using the vdW-DF method in versions vdW-DF-cx, vdW-DF1, and vdW-DF2. All results are for the optimal configuration, and for xylene and tri-methylbenzene we choose the structural isomer that has its methyl groups evenly distributed around the aromatic ring (para-xylene and mesitylene).

for small molecules, like the G22 set of molecules [36] and other systems with atoms or small molecules. It has been shown to work well for such systems [8, 37–39]. However, part of the system considered here is an extended system (graphene) which was not a target system for the development of vdW-DF2. In vdW-DF-cx the exchange functional is chosen so as to match the inner functional [9, 35] and to observe important physics rules. In general, vdW-DF-cx improves the adsorption distances and energies compared to vdW-DF1. As previously seen in adsorption systems [10, 40], the vdW-DF-cx provides larger overall binding energies than for vdW-DF1, here with energies 0.08–0.12 eV larger per molecule (Table I).

The adsorption energies  $E_a$  of Table I are plotted in Figure 4 as a function of growing number of methyl groups, for the ‘edge’ configuration of the H tripods. We see that the increase in  $E_a$  is almost linear with number of methyl groups, with an offset, corresponding to the adsorption energy of benzene, Table I. For each methyl group added an H atom is also removed, thus the net gain of atoms is one C and two H atoms. One of us found in an earlier study [18], by use of vdW-DF1, that in adsorption of the linear n-alkanes on graphene the gain in adsorption energy per additional  $\text{CH}_2$  group added to the length of the alkane molecule is 0.075 eV. This fits reasonably well with the increase found here when we use vdW-DF1:  $E_a$  increases by 0.090 eV per added methyl group. For the vdW-DF-cx calculations the corresponding increase is also approximately 0.09 eV per methyl group, while the vdW-DF2 results vary more and are generally 0.04–0.06 eV smaller than the vdW-DF1 results. The rather systematic increase per added methyl group for vdW-DF-cx and vdW-DF1 suggests that in modeling systems with large or many molecules, the methyl group may be

modeled as an entity.

The unit cell in the calculations contains one molecule, in addition to graphene. However, because of the periodic boundary conditions each molecule has neighbors at approximately 12 Å distance (the length of the sides of the unit cell). This is far from full coverage. In Ref. [28] the area occupied by an adsorbed toluene molecule on graphite is measured to be 46 Å<sup>2</sup>. In our orthorhombic unit cell of lateral size 12.9 Å × 12.4 Å area one molecule per unit cell thus leads to an estimated coverage 0.29 ML. In Ref. [41], on the other hand, Monte Carlo simulations are used to find the coverage concentration 4.30 μmol/m<sup>2</sup>, which corresponds to an area per molecule 38.6 Å<sup>2</sup>. From this number, we can estimate our coverage to approximately 0.24 ML, in any case far from full coverage.

At sparse coverages, such as here, it is favorable for the relatively flat methylbenzenes to orient the aromatic ring approximately parallel to graphene, in order to maximize the area of interaction. On the other hand, at high coverages, the total interaction with graphene and with neighboring molecules is maximized if the molecules tilt or stand up perpendicular to graphene. This was shown for close to full coverage in empirical Monte Carlo simulations of benzene, toluene, and para-xylene on graphene [41], and in experiments for other flat molecules in Ref. [31]. At a coverage of approximately 0.24–0.29 ML the molecules in our calculations are expected to benefit energetically from being in a position parallel to graphene, which is the orientation we consider here.

Optimizing how the methylbenzenes are positioned relative to graphene there are several minima in the binding energy. As described in the previous section, the (center of) the aromatic ring can be positioned on top of a graphene C atom (‘top’), on top of an aromatic ring in graphene (‘hollow’), on top of the bridge between two nearest-neighbor graphene C atoms (‘bridge’), or any position in between these. The ring can be rotated around its center and thus change the position of the methyl-group C atom(s) relative to graphene. Further, the methyl group H-atom tripod can be rotated around its C atom such as to have one or two H-atoms pointing towards graphene. Several of these changes in positions are surveyed in the Supplemental material, here we extract and discuss their energy differences.

As explained in the results section, the ‘edge’ orientation of the methyl group is preferable, gaining 22–38 meV per methyl group compared to the ‘corner’ orientation. This is natural, as by having the H-tripod edges pointing to graphene the whole molecule can move closer to graphene, and it thus obtains a slightly larger adsorption energy.

Comparing the position of the aromatic ring relative to graphene, with everything else kept the same, we find that the ‘top’ or ‘bridge’ position is most favorable. Changing the ring position to the ‘hollow’ position comes at a cost of about 20 meV. As found for chloroform on graphene [16], the energy difference for the various ad-

sorption sites is small, and the corrugation of graphene also for the methylbenzenes studied here is so small that it only takes little kinetic energy to overcome the energy barriers for moving along graphene once the molecule is adsorbed on graphene. At room temperature the methylbenzenes are free to move, both translational and rotational.

We previously reported the results of toluene on graphene, by use of vdW-DF1, obtained by visiting high school students who worked in a research project in our group [27]. For time reasons the students used a lower quality on the convergence parameters, they used the ‘corner’ orientation of the methyl H-tripod, and they did not explore the energy landscape of various positions and orientations of toluene on graphene. However, toluene was (as here) placed with the aromatic ring parallel to graphene and atomic positions were allowed to relax locally. The students obtained the adsorption energy 0.479 eV per molecule, whereas the present study gives adsorption energies for toluene in orientation ‘corner’ in the range 0.476–0.498 eV, using vdW-DF1 for their calculations (Table I). Thus, the lower accuracy of the students’ calculations only affected the binding energy by 0.01–0.02 eV (1–2 kJ/mol), or less than 4%, compared to higher accuracy in the present study.

In an early stage of the vdW-DF development one of us calculated the adsorption energy of benzene on graphene, using vdW-DF1 but without local optimization of atomic positions. The DFT code used was dacapo in a locally supplied non-selfconsistent version for the dispersion interaction in vdW-DF1, used after a consistent GGA calculation of the electron density. Those calculations showed an adsorption energy for benzene 0.495 eV (0.763 eV for naphthalene) [12].

For toluene and benzene experimental measurements of the heat of adsorption are available from Refs. [28–30], included in Table I. The values indicate that the calculated results are reasonable, taking into account that the experiments are for systems that are not in vacuum, are at non-zero temperature, and measured at approximately one monolayer (ML) coverage, much denser than the present calculations. In Ref. [27] we estimated the zero-point motion of toluene to be just a few meV, which we can therefore ignore here.

In the calculations presented here the adsorption systems are in vacuum, which is not the situation in water or air filters. One of us has earlier studied how the presence

of water molecules affects the adsorption results of, e.g., chloroform on graphene or graphene oxide [16, 42]. As argued in Ref. [42], if the adsorption energy is affected by water, that effect can only show in the part of the energy containing the nonlocal part of the correlation interaction. On the other hand, that nonlocal part of the energy is found as a sum of poles in a contour integral in the space of complex frequencies, the sum starting at frequencies much higher than the range where the index of refraction for water differs from unity. The water molecules do not engage in the vibrations and thus do not change the nonlocal interaction.

## VI. SUMMARY

We report on a density functional study of methylbenzenes adsorbed on graphene. We find that although some adsorption configurations are energetically better than others, the energy differences are all small. Changing the orientation of the H tripod on the methyl group(s) of the molecules gives rise to the largest energy difference, which is approximately in the range 22–38 meV per methyl group, followed by the positioning of the center of the aromatic ring on graphene, showing a difference of only 20 meV, which means that at room temperature this difference can be ignored. Rotations around the center of the aromatic ring are so small (8 meV or less) that they may be ignored entirely, even at low temperature. Including also benzene in the study we show that the adsorption energy per molecule increases approximately linearly with number of methyl groups in the molecule. We use the vdW-DF method, mainly in the original version vdW-DF1, but we also use the vdW-DF-cx and vdW-DF2 versions. As expected, the adsorption energies differ between these, with the most reliable method vdW-DF-cx yielding the largest adsorption energies.

## ACKNOWLEDGMENTS

Support from the Swedish Research Council (VR) is gratefully acknowledged. The computations were in part performed on resources at Chalmers Centre for Computational Science and Engineering (C3SE) provided by the Swedish National Infrastructure for Computing (SNIC).

- 
- [1] M. L. Terranova, S. Orlanducci, and M. Rossi, eds., *Carbon Nanomaterials for Gas Adsorption* (CRC Press, 2012).
  - [2] S. Mao, J. Chang, G. Zhou, and J. Chen, *Small* **11**, 5336 (2015).
  - [3] V. C. Sanchez, A. Jachak, R. H. Hurt, and A. B. Kane, *Chem. Res. Toxicol.* **25**, 15 (2012).
  - [4] S. M. Maliyekkal, T. S. Sreeprasad, D. Krishnan, S. Kouser, A. K. Mishra, U. V. Waghmare, and T. Pradeep, *Small* **9**, 273 (2013).
  - [5] M. Dion, H. Rydberg, E. Schröder, D. C. Langreth, and B. I. Lundqvist, *Phys. Rev. Lett.* **92**, 246401 (2004).
  - [6] M. Dion, H. Rydberg, E. Schröder, D. C. Langreth, and B. I. Lundqvist, *Phys. Rev. Lett.* **95**, 109902 (2005).

- [7] T. Thonhauser, V. R. Cooper, S. Li, A. Puzder, P. Hyldgaard, and D. C. Langreth, *Phys. Rev. B* **76**, 125112 (2007).
- [8] K. Lee, È. D. Murray, L. Kong, B. I. Lundqvist, and D. C. Langreth, *Phys. Rev. B* **82**, 081101 (2010).
- [9] K. Berland and P. Hyldgaard, *Phys. Rev. B* **89**, 035412 (2014).
- [10] K. Berland, C. A. Arter, V. R. Cooper, K. Lee, B. I. Lundqvist, E. Schröder, T. Thonhauser, and P. Hyldgaard, *J. Chem. Phys.* **140**, 18A539 (2014).
- [11] K. Berland, V. R. Cooper, K. Lee, E. Schröder, T. Thonhauser, P. Hyldgaard, and B. I. Lundqvist, *Rep. Prog. Phys.* **78**, 066501 (2015).
- [12] S. D. Chakarova-Käck, E. Schröder, B. I. Lundqvist, and D. C. Langreth, *Phys. Rev. Lett.* **96**, 146107 (2006).
- [13] S. D. Chakarova-Käck, Ø. Borck, E. Schröder, and B. I. Lundqvist, *Phys. Rev. B* **74**, 155402 (2006).
- [14] K. Berland, S. D. Chakarova-Käck, V. R. Cooper, D. C. Langreth, and E. Schröder, *J. Phys.: Condens. Matter* **23**, 135001 (2011).
- [15] D. Le, A. Kara, E. Schröder, P. Hyldgaard, and T. S. Rahman, *J. Phys.: Condens. Matter* **24**, 424210 (2012).
- [16] J. Åkesson, O. Sundborg, O. Wahlström, and E. Schröder, *J. Chem. Phys.* **137**, 174702 (2012).
- [17] E. Schröder, *J. Nanomater.* **2013**, 871706 (2013).
- [18] E. Londero, E. K. Karlson, M. Landahl, D. Ostrovskii, J. D. Rydberg, and E. Schröder, *J. Phys.: Condens. Matter* **24**, 424212 (2012).
- [19] R. F. White and S. P. Proctor, *Lancet* **349**, 1239 (1997).
- [20] “Open-source, grid-based PAW-method DFT code GPAW,” <http://wiki.fysik.dtu.dk/gpaw/> (2016).
- [21] J. Enkovaara, C. Rostgaard, J. J. Mortensen, J. Chen, M. Dułak, L. Ferrighi, J. Gavnholt, C. Glinsvad, V. Haikola, H. A. Hansen, H. H. Kristoffersen, M. Kuisma, A. H. Larsen, L. Lehtovaara, M. Ljungberg, O. Lopez-Acevedo, P. G. Moses, J. Ojanen, T. Olsen, V. Petzold, N. A. Romero, J. Stausholm-Møller, M. Strange, G. A. Tritsarlis, M. Vanin, M. Walter, B. Hammer, H. Häkkinen, G. K. H. Madsen, R. M. Nieminen, J. K. Nørskov, M. Puska, T. T. Rantala, J. Schiøtz, K. S. Thygesen, and K. W. Jacobsen, *J. Phys.: Condens. Matter* **22**, 253202 (2010).
- [22] S. R. Bahn and K. W. Jacobsen, *Comput. Sci. Eng.* **4**, 56 (2002).
- [23] “Python-based atomic simulation environment ASE,” <https://wiki.fysik.dtu.dk/ase/> (2016).
- [24] “Open-source DFT code QE,” <http://www.quantum-espresso.org/> (2016).
- [25] P. Giannozzi, S. Baroni, N. Bonini, M. Calandra, R. Car, C. Cavazzoni, D. Ceresoli, G. L. Chiarotti, M. Cococcioni, I. Dabo, A. D. Corso, S. Fabris, G. Fratesi, S. de Gironcoli, R. Gebauer, U. Gerstmann, C. Gougousis, A. Kokalj, M. Lazzeri, L. Martin-Samos, N. Marzari, F. Mauri, R. Mazzarello, S. Paolini, A. Pasquarello, L. Paulatto, C. Sbraccia, S. Scandolo, G. Sclauzero, A. P. Seitsonen, A. Smogunov, P. Umari, and R. M. Wentzcovitch, *J. Phys.: Condens. Matter* **21**, 395502 (2009).
- [26] G. Román-Pérez and J. M. Soler, *Phys. Rev. Lett.* **103**, 096102 (2009).
- [27] J. Ericsson, T. Husmark, C. Mathiesen, B. Sepahvand, Ø. Borck, L. Gunnarsson, P. Lydmark, and E. Schröder, “Involving high school students in computational physics university research: Theory calculations of toluene adsorbed on graphene,” (2016), preprint.
- [28] M. Monkenbusch and R. Stockmeyer, *Ber. Bunsenges. Phys. Chem.* **85**, 442 (1981).
- [29] H. Ulbricht, R. Zacharia, N. Cindir, and T. Hertel, *Carbon* **44**, 2931 (2006).
- [30] R. Zacharia, H. Ulbricht, and T. Hertel, *Phys. Rev. B* **69**, 155406 (2004).
- [31] C.-M. Grimaud, D. Radosavkic, S. Ustaze, and R. Palmer, *Applied Surface Science* **178**, 1 (2001).
- [32] S. D. Chakarova and E. Schröder, *J. Chem. Phys.* **122**, 054102 (2005).
- [33] S. D. Chakarova-Käck, A. Vojvodic, J. Kleis, P. Hyldgaard, and E. Schröder, *New J. Phys.* **12**, 013017 (2010).
- [34] Y. Zhang and W. Yang, *Phys. Rev. Lett.* **80**, 890 (1998).
- [35] P. Hyldgaard, K. Berland, and E. Schröder, *Phys. Rev. B* **90**, 075148 (2014).
- [36] L. Curtiss, K. Raghavachari, G. W. Trucks, and J. A. Pople, *J. Chem. Phys.* **94**, 7221 (1991).
- [37] K. Lee, Y. Morikawa, and D. C. Langreth, *Phys. Rev. B* **82**, 155461 (2010).
- [38] K. Lee, A. K. Kelkkanen, K. Berland, S. Andersson, D. C. Langreth, E. Schröder, B. I. Lundqvist, and P. Hyldgaard, *Phys. Rev. B* **84**, 193408 (2011).
- [39] D. L. Chen, W. A. Al-Saidi, and J. K. Johnson, *J Phys: Condens Matter* **24**, 424211 (2012).
- [40] T. Thonhauser, S. Zuluaga, C. A. Arter, K. Berland, E. Schröder, and P. Hyldgaard, *Phys. Rev. Lett.* **115**, 136402 (2015).
- [41] N. Klomkliang, D. D. Do, and D. Nicholson, *Industrial and Engineering Chemical Research* **51**, 5320 (2012).
- [42] E. Kuisma, C. F. Hansson, T. B. Lindberg, C. A. Gillberg, S. Idh, and E. Schröder, *J. Chem. Phys.* **144**, 184704 (2016).